MILITARY TECHNICAL COLLEGE
CAIRO - EGYPT

7th INTERNATIONAL CONF. ON
AEROSPACE SCIENCES &
AVIATION TECHNOLOGY

Dynamic Behavior of Improved Compact Signature Analysis Based on LFSR

Prof. Dr. SAID GHONIEMY **
Faculty of Computer Science and Information Systems
Ain Shams University

Abstract :

In compact signature analysis (CSA) using Linear Feedback Shift Registers (LFSR), one unit connected in a closed loop form with the Circuit Under Test (CUT) is used as a random test pattern generator and signature analyzer in the same time; thus, reducing the hardware of signature analysis testing technique by 50 % [10]. However, it was found that the Steady State Aliasing Error Probability (SS-AEP) of CSA has values between 0 and 1 depending on the CUT and the structure of the CSA; which inhibits its use for digital circuits testing. In a previous work, the hardware condition for the SS-AEP of CSA to be equal to $/2^k$ is obtained, leading to what is called the Improved Compact Signature Analysis (ICSA) [11].

In this paper, the dynamic behavior of the CSA and the ICSA, which reflects the minimum required length of the test pattern necessary for the compression technique to reach SS-AEP condition is studied, using the absolute value of the Second Maximum Eigenvalues (SME) of transition probability matrix (TPM). The results are compared with those of Open Loop testing systems with PP-LFSR, and Cyclic Code Linear Feedback Shift Register (CC-LFSR). The comparison indicates that when the probability of the system to be fault-free is equally likely, the ICSA has similar dynamic performance as the conventional testing systems, but in the general case, the ICSA needs shorter pattern than CC-LFSR and slightly longer pattern than PP-LFSR in conventional testing to reach steady state, and as k increases the difference between the dynamic behavior of the ICSA and PP-LFSR decreases.

---

* Professor, Faculty of Computer Science & Information Systems, Ain Shams University.

1.0 Introduction :

In digital circuits, testing is carried out by applying a sequence of input stimuli, known as *test vectors,* generated by Test Pattern Generator (TPG), and checking for possible faults in the circuit by observing the circuit response at primary outputs. A general diagnosis system for digital-circuits comprises a TPG, that cycles through the whole or sufficiently large portion of input space, stimulating the CUT. The output of that circuit is then compressed using Data Compressor (DC) generating the circuit signature. This signature is then compared against a known one (REF), where a judgment can be made about the correctness of the circuit. The system is composed of our main blocks : TPG, DC, Comparator, and Storage for reference signature as shown in Fig. 1.

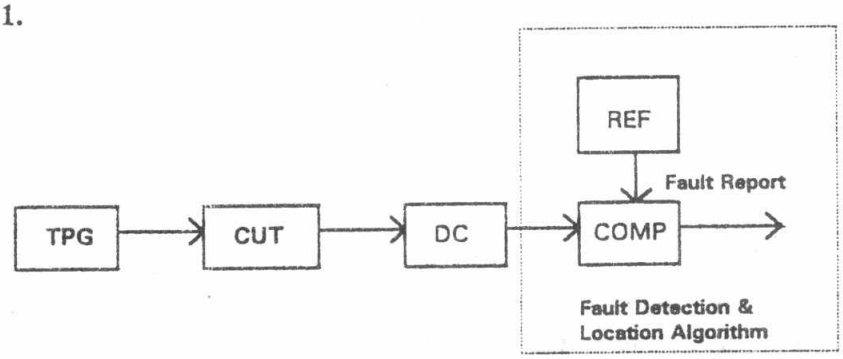

Fig. 1 Digital circuits diagnosis system block diagram.

The signature algorithm should not lose information. Specifically it must not lose that evidence of a fault indicated by a wrong response from CUT. This is referred to as *Masking* (Aliasing Error Probability) effect which is the compression of an erroneous output sequence from a faulty circuit into the same signature as the fault free circuit. Masking detracts from the quality of the test, in sense that the input pattern have detected a fault but the act of compression hides it. An important measure of good compression technique is how well it minimizes the masked errors.

Linear Feedback Shift Registers (LFSR) are used extensively in Testing of digital circuits, and built-in Self Testing (BIST) design; as a source of pseudorandom binary test vector, and as a means to carry out response compression - known as *signature analysis,* to determine pass or fail status. This leads to the idea of compact signature analyzer (CSA), in which one unit, connected in a closed loop form with the CUT, is used as a random test pattern generator and signature analyzer in the same time, as shown in Fig. 2. This procedure reduces the hardware of signature analysis testing technique by 50 %.

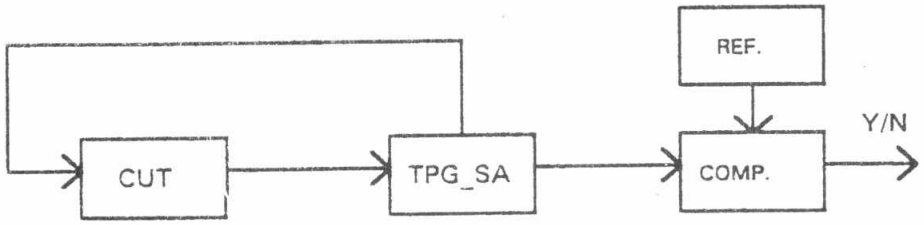

Fig. 2 CSA block diagram.

The general functional diagram of the CSA using LFSR is shown in Fig. 3.

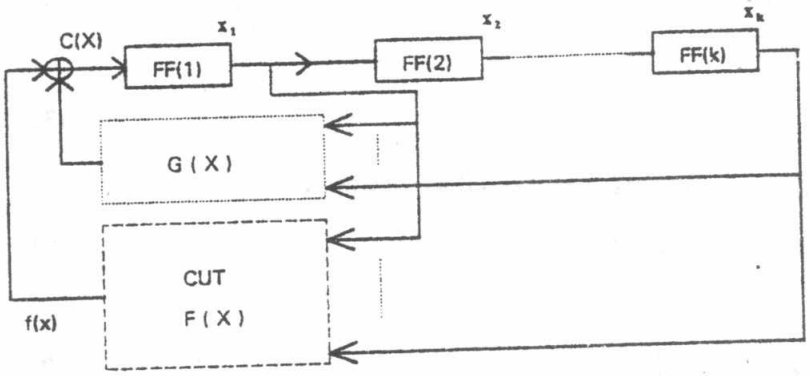

Fig. 3 The general construction of the CSA using LFSR.

The steady state behavior of the Compact Signature Analysis (CSA) with LFSR has been studied [10],[11]. The preliminary results indicated that the aliasing error probability has values between 0 and 1 depending on the CUT, and the construction of the CSA, which prohibits its use for digital circuit testing. The hardware conditions for the SS-AEP to be equal to 2^{-k} is obtained, leading to what is called the Improved Compact Signature Analysis (ICSA), shown in Fig. 4. The theoretical analysis and simulation results indicated that the 2^{-k} error limit is attainable iff the k^{th} stage of the CSA is not connected to any of the inputs of the CUT.

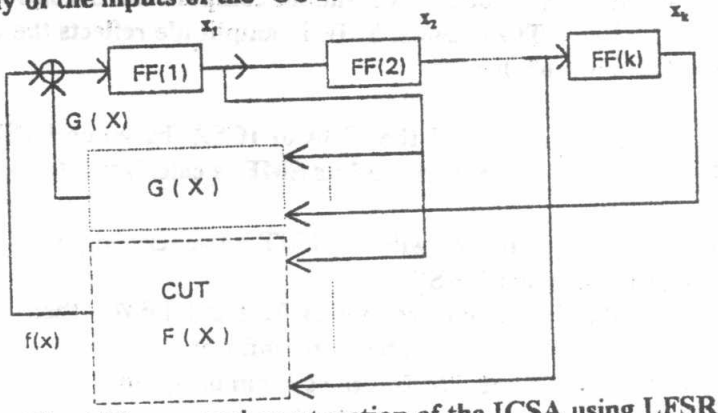

Fig. 4 The general construction of the ICSA using LFSR.

This paper, deals with the dynamic behavior of CSA and ICSA with LFSR which reflects the minimum required length of the test pattern necessary for the compression technique to reach the SS-AEP condition. The absolute value of the maximum eigenvalues of transition probability matrix (TPM) representing the simulated system is calculated [1]. Since the maximum eigenvalue for any Markov process of the TPM is equal to one [1], [2], [3], therefore, the Second Maximum Eigenvalue (SME) of the TPM representing the CSA is considered. The obtained results are compared with those of open loop compaction based on LFSR and CC-LFSR.

2.0 Dynamic Properties of Markov Processes :

The multi-step Transition Probability Matrix (TPM) $\phi(n)$ is equal to the n^{th} power of TPM (P) [1].

$$\phi(n) = P^n \qquad \text{for } n = 0,1,2,.... \qquad (1)$$

The Z- transform is used to study the dynamic properties of Markov process systems as follows[2] :

$$F(Z)=\sum_{n=0} f(n)\ Z^{-n} \tag{2}$$

Let us define

$$\phi(n+1)=\phi(n)\ \underline{P} \tag{3}$$

The corresponding Z - transform is expressed as follows :

$$Z(\phi(Z)-\phi(0))=\phi(Z)\ \underline{P} \tag{4}$$

then

$$\phi(Z)=\phi(0)\ Z\ (Z\ \underline{I}-\underline{P})^{-1} \tag{5}$$

thus

$$\phi(n)=\phi(0)\ F^{-1}(Z(Z\ \underline{I}-\underline{P})^{-1}) \tag{6}$$

$$=\phi(0)\ \underline{P}$$

The locations of the zeros of the denominator of the inverse matrix controls the dynamic properties of the solution. The first maximum eigen value (zeros of the characteristic equation) for TPM is equal to one [1], therefore, to compare between two systems modeled by Markov process, we should compare the Second Maximum Eigen value (SME) of the TPM. The greatest SME in amplitude reflects the compaction need for longest pattern (number of clocks).

To study the performance of the CSA or ICSA based on LFSR, the proposed system is modelled as a Markov process, and its SME is calculated through :

- **Modeling the CSA connected with the CUT by generating the Markov State Diagram (MSD).**
- **Constructing the Transition Probability Matrix (TPM), then Multiplying it n times, where n tends to infinity.**
- **Deducing the equation of SME of the system using [8].**
- **Plotting the results, and analyzing the behavior.**

3.0 Modeling of the Dynamic Behavior (DB) for CSA and ICSA :

Let P_{ij} be the probability of transition from state i to state j in one step, and let it be constant. That is , it doesn't matter at what time one enters state i , the probability of going to state j is always P_{ij}.

A Markov process can be described by the transition matrix $\underline{P}=[P_{ij}]$. This process is called stationary if P_{ij} is not a function of when one arrives in state i. A transition from one of these states to the actual state coincides with faulty or non faulty paths. The probabilities for these transitions are p and 1-p respectively. The following sections discuss the SME of TPM for different cases :

A) CSA with LFSR :

1- CSA with LFSR where the k outputs of the signature analyzer are connected to the m inputs of CUT (for both PP and NPP).

2- CSA with LFSR, k > m, and Last Stage of signature analyzer connected to one of the inputs of CUT

B) ICSA with LFSR : Where k > m, and signature analyzer output Last Stage Not Connected (LSNC) to any of the inputs of CUT for both PP-LFSR and NPP-LFSR.

3.1 DB for CSA Structure with k = m :

The cases in which all the outputs of the LFSR stages are connected to the inputs of the CUT have been studied as follows :

3.3.1 DB for CSA Structure with LFSR, PP, k = m = 2, CUT(1) :

Fig. 5 presents the CSA composed of a 2-stage PP-LFSR, a 2-input AND gate as the CUT(1). The outputs of the 2-stage LFSR are connected to the inputs of the CUT(1), and the output of the CUT(1) is fedback to the first stage of LFSR through an XOR circuit. Fig. 6 represents the MSD of the system in Fig. 5. The TPM for the system is shown in Fig. 7

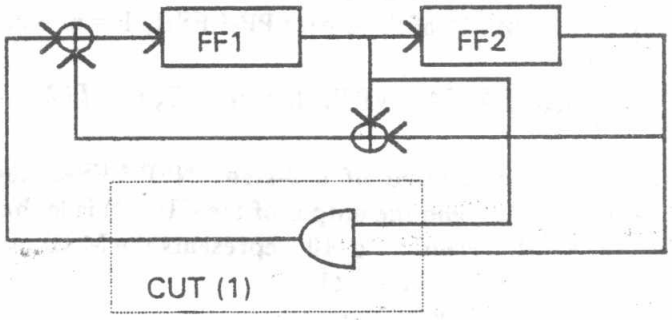

Fig. 5. Structure for CSA, LFSR, PP, with k = m =2, CUT(1).

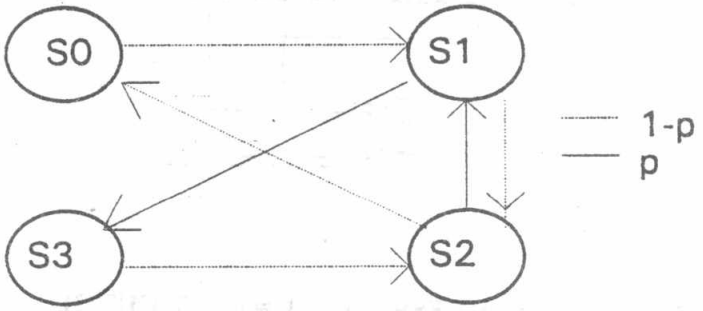

Fig. 6. MSD for CSA, LFSR, PP, with k = m = 2, CUT(1).

M1 =

	s_0	s_1	s_2	s_3
s_0	p	1-p	0	0
s_1	0	0	1-p	p
s_2	1-p	p	0	0
s_3	0	0	1-p	p

Fig. 7. TPM for LFSR, PP, with k = m =2, CUT(1).

The SME for the TPM M1 is calculated with [8]; giving :

$$SME1 = p - \frac{1}{2} + \frac{1}{2}\sqrt{-4p^2 + 8p - 3} \qquad (7)$$

The absolute value SME1 is plotted against p as shown in Fig. 8. It equals zero for the case of equally likely error model when p = q = 0.5, and equals one for p = 0 or p = 1 .

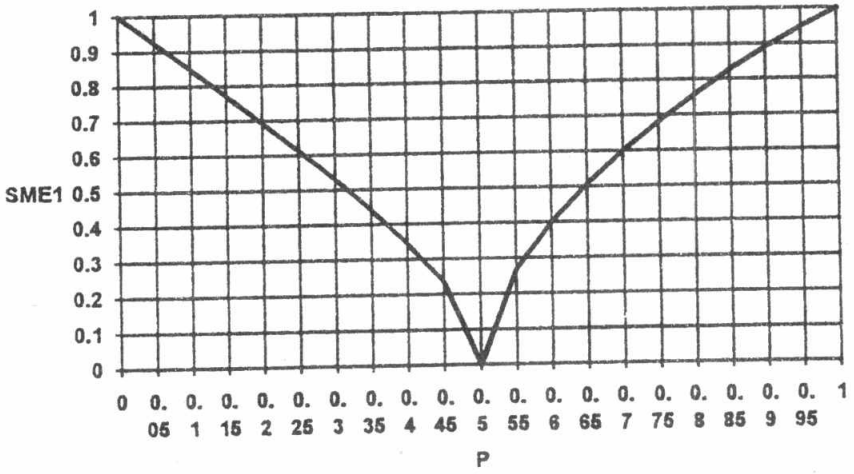

Fig. 8. Dependence of the absolute values of SME1 upon error probability of CUT (1) for TPM M1 of CSA with PP-LFSR, k = m = 2.

3.3.2 Structure of CSA with LFSR, NPP, k = m = 3, CUT(2) :

Fig. 9. presents the CSA composed of a 3-stage NPP-LFSR. the outputs are connected to the inputs of the CUT(2), and the output of the CUT(2) is fedback to the first stage of LFSR through an XOR circuit. Fig. 10 represents the MSD of the system in Fig. 9. The TPM for the system is shown in Fig.11.

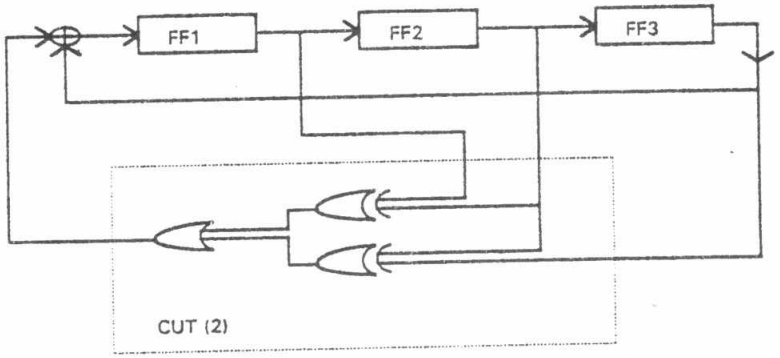

Fig. 9. CSA with LFSR, NPP, k = m = 3, CUT(2).

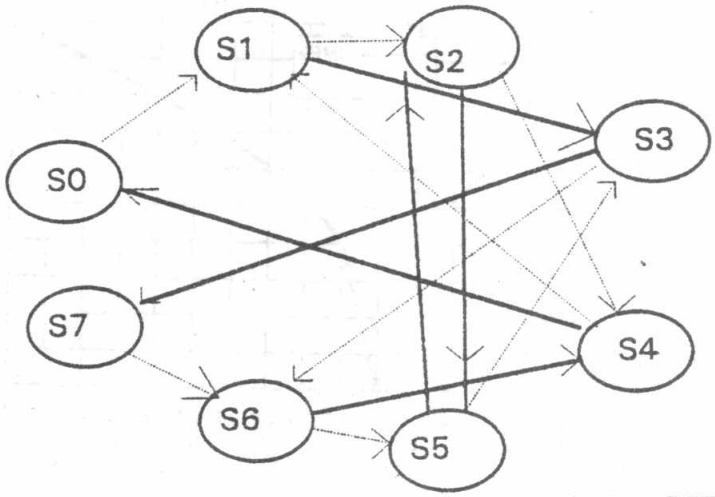

Fig.10. MSD for CSA with LFSR, NPP, k = m = 3, CUT (2).

$$M2 = \begin{array}{c|cccccccc} & s_0 & s_1 & s_2 & s_3 & s_4 & s_5 & s_6 & s_7 \\ s_0 & p & 1-p & 0 & 0 & 0 & 0 & 0 & 0 \\ s_1 & 0 & 0 & 1-p & p & 0 & 0 & 0 & 0 \\ s_2 & 0 & 0 & 0 & 0 & 1-p & p & 0 & 0 \\ s_3 & 0 & 0 & 0 & 0 & 0 & 0 & 1-p & p \\ s_4 & p & 1-p & 0 & 0 & 0 & 0 & 0 & 0 \\ s_5 & 0 & 0 & p & 1-p & 0 & 0 & 0 & 0 \\ s_6 & 0 & 0 & 0 & 0 & p & 1-p & 0 & 0 \\ s_7 & 0 & 0 & 0 & 0 & 0 & 0 & 1-p & p \end{array}$$

Fig. 11. TPM for CSA with LFSR, NPP, k = m = 3, CUT (2).

The SME for the TPM M2 is calculated with [8], giving :

$$SME2 = -\frac{1}{36}.2^{\left(\frac{1}{3}\right)}.3^{\left(\frac{2}{3}\right)}.\frac{a}{b} \qquad (8)$$

where

$$a = \left[\begin{array}{l} \left(18p^2-27p+9-i.\sqrt{8p^4-4p^3-27p^2+54p-27}.\sqrt{3}+2i.\sqrt{8p^4-4p^3-27p^2+54p-27}.\sqrt{3}.p\right)^{\left(\frac{2}{3}\right)}.2^{\left(\frac{1}{3}\right)}.3^{\left(\frac{2}{3}\right)}-6p+ \\ 12p^2-3i.3^{\left(\frac{1}{6}\right)}.\left(18p^2-27p+9-i.\sqrt{8p^4-4p^3-27p^2+54p-27}.\sqrt{3}+2i.\sqrt{8p^4-4p^3-27p^2+54p-27}.\sqrt{3}.p\right)^{\left(\frac{2}{3}\right)}. \\ 2^{\left(\frac{1}{3}\right)}-6i.\sqrt{3}.p+12i.\sqrt{3}.p^2 \end{array}\right]$$

and

$$b = \left(18p^2-27p+9-i.\sqrt{8p^4-4p^3-27p^2+54p-27}.\sqrt{3}+2i.\sqrt{8p^4-4p^3-27p^2+54p-27}.\sqrt{3}.p\right)^{\left(\frac{1}{3}\right)}$$

The absolute value of SME2 is plotted against p as shown in Fig. 12. It equals to zero for the case of equally likely error model when p = q = 0.5, and equals one for p = 0 or p = 1 .

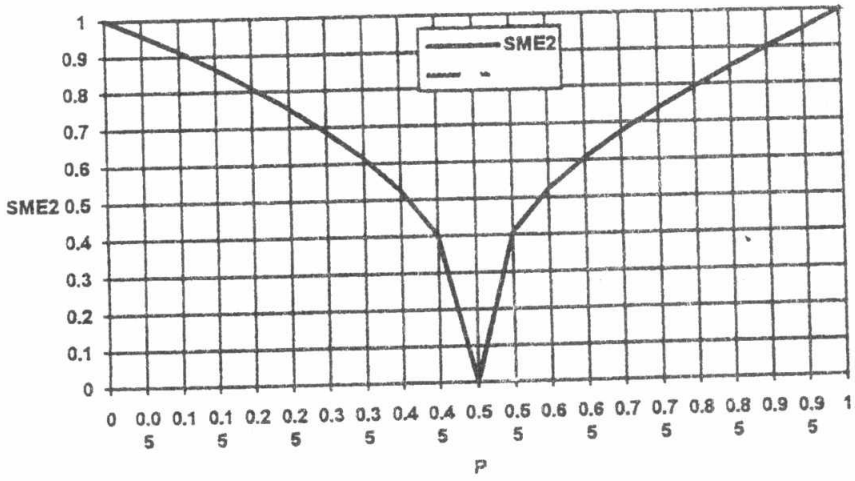

Fig. 12. Dependence of the absolute values of SME2 upon error probability of CUT (2) for TPM M2 of CSA with NPP-LFSR, k = m = 3.

3.2 DB for CSA Structure with k > m, with Connecting Last Stage (CLS) :

3.2.1 DB for CSA Structure with LFSR, PP, k = 3, m = 2, CUT(3) :

Fig. 13. presents the CSA composed of a 3-stage PP-LFSR, two of the outputs, including the last stage output, are connected to the CUT (3) inputs, and the output of the CUT(3) is fedback to the first stage of LFSR through an XOR circuit. Fig. 14. represents the MSD of the system in Fig. 13. The TPM for the system is shown in Fig. 15.

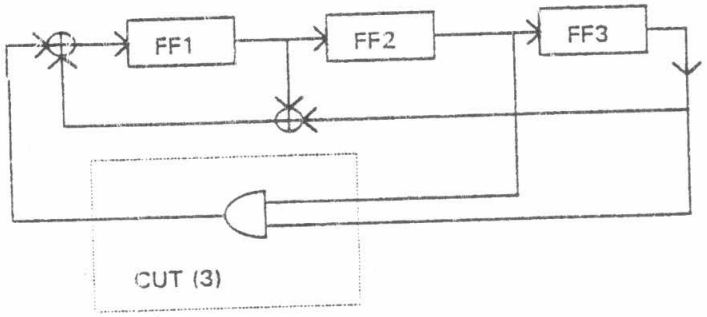

Fig. 13 CSA with LFSR, PP, k = 3, m = 2, CLS, CUT(3).

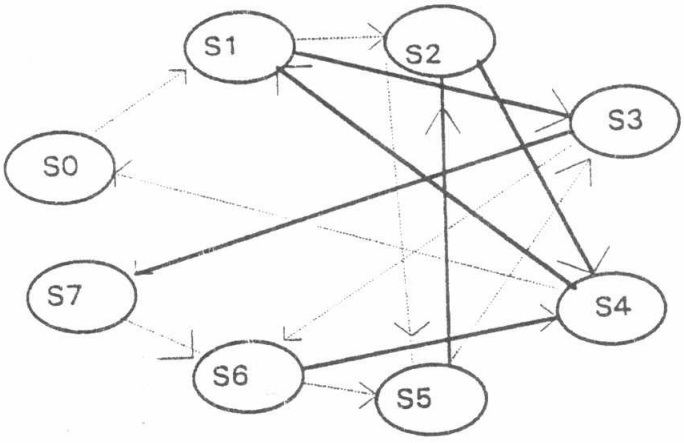

Fig. 14. MSD for CSA with LFSR, PP, k = 3, m = 2, CLS, CUT(3).

$$M3 = \begin{array}{c|cccccccc} & s_0 & s_1 & s_2 & s_3 & s_4 & s_5 & s_6 & s_7 \\ s_0 & p & 1-p & 0 & 0 & 0 & 0 & 0 & 0 \\ s_1 & 0 & 0 & 1-p & p & 0 & 0 & 0 & 0 \\ s_2 & 0 & 0 & 0 & 0 & p & 1-p & 0 & 0 \\ s_3 & 0 & 0 & 0 & 0 & 0 & 0 & 1-p & p \\ s_4 & 1-p & p & 0 & 0 & 0 & 0 & 0 & 0 \\ s_5 & 0 & 0 & p & 1-p & 0 & 0 & 0 & 0 \\ s_6 & 0 & 0 & 0 & 0 & p & 1-p & 0 & 0 \\ s_7 & 0 & 0 & 0 & 0 & 0 & 0 & 1-p & p \end{array}$$

Fig. 15. TPM for CSA with LFSR, PP, k = 3, m = 2, CLS, CUT(3).

The SME for the TPM M3 is calculated with [8]; giving :

$$SME3 = p - \frac{1}{2} + \frac{1}{2}.\sqrt{-4p^2 + 8p - 3} \qquad (9)$$

The absolute value SME3 is plotted against p as shown in Fig.16. It equals zero for the case of equally likely error model when p = q = 0.5, and equals one for p = 0 or p = 1 .

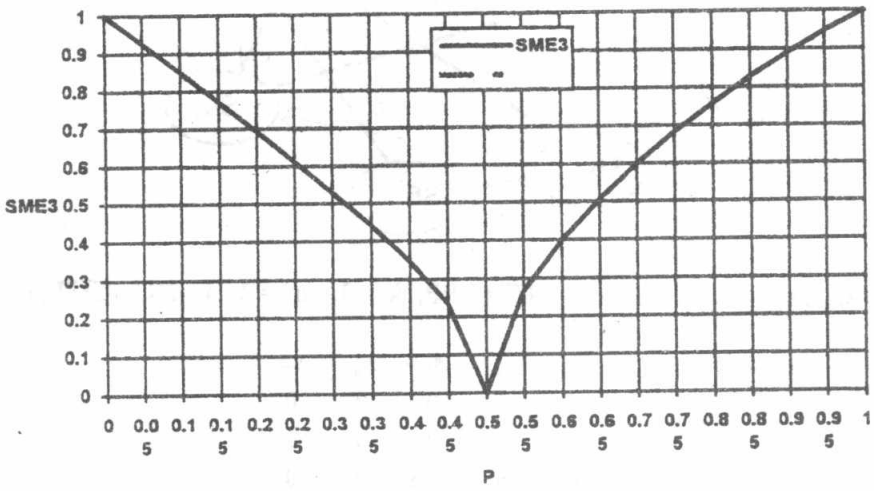

Fig. 16. Dependence of the absolute values of SME3 upon error probability of CUT (3) for TPM M3 of CSA with PP-LFSR, k = 3, m = 2.

3.3 DB for ICSA Structure (with k > m, with Last Stage Not Connected (LSNC)) :

The cases in which last stage output of the LFSR is not connected to any of the CUT inputs, have been studied as follows :

3.3.1 DB for CSA Structure with LFSR, PP, k= 3, m = 2, LSNC, CUT(4) :

Fig. 17. presents the CSA composed of a 3-stage PP-LFSR, two outputs - not including the last stage one - are connected to the CUT (4) inputs, and the output of the CUT(4) is fedback to the first stage of LFSR through an XOR circuit. Fig. 18 represents the MSD of the system in Fig. 17. The TPM for the system is shown in Fig. 19.

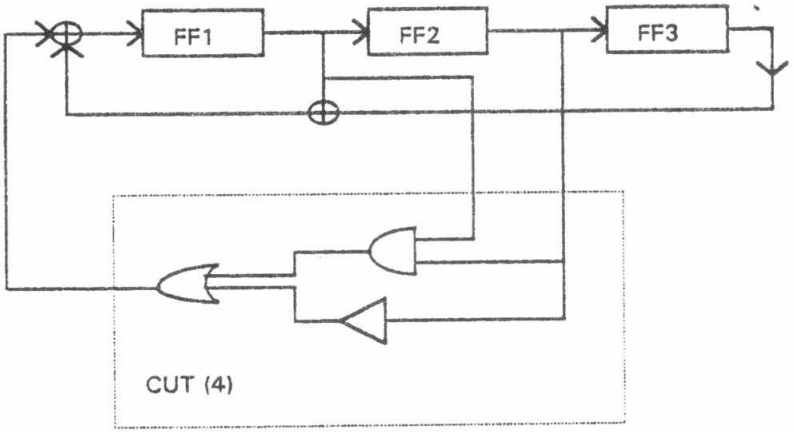

Fig. 17. CSA with LFSR, PP, k = 3, m = 2, LSNC, CUT(4).

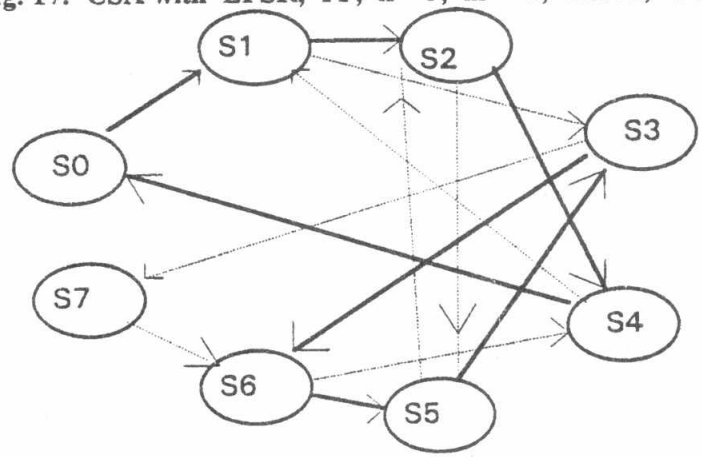

Fig. 18. MSD for CSA with LFSR, PP, k = 3, m = 2, LSNC, CUT(4).

M4 =	s_0	s_1	s_2	s_3	s_4	s_5	s_6	s_7
s_0	1-p	p	0	0	0	0	0	0
s_1	0	0	p	1-p	0	0	0	0
s_2	0	0	0	0	p	1-p	0	0
s_3	0	0	0	0	0	0	p	1-p
s_4	p	1-p	0	0	0	0	0	0
s_5	0	0	1-p	p	0	0	0	0
s_6	0	0	0	0	1-p	p	0	0
s_7	0	0	0	0	0	0	1-p	p

Fig. 19. TPM for CSA with LFSR, PP, k = 3, m = 2, LSNC, CUT(4).

The SME for the TPM M4 is calculated with [8]; giving :

$$SME4 = \sqrt{1-2p} \qquad (10)$$

The absolute value of SME4 is plotted against p as shown in Fig. 20. It equals zero for the case of equally likely error model when $p = q = 0.5$, and equals one for $p = 0$ or $p = 1$.

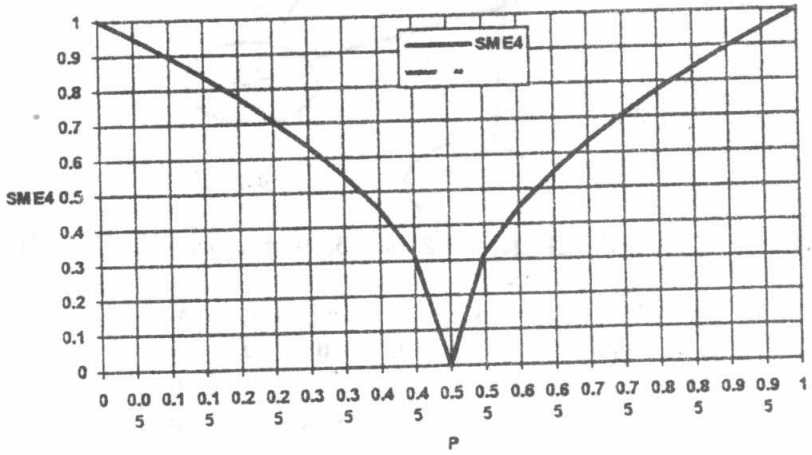

Fig. 20. Dependence of the absolute values of SME4 upon error probability of CUT (4) for TPM M4 of CSA with PP-LFSR, k = 3, m = 2, LSNC.

3.3.2 DB for CSA Structure with LFSR, NPP, k = 3, m = 2, LSNC,CUT(5) :

Fig. 21. presents the CSA composed of a 3-stage NPP-LFSR, two outputs - not including the last stage one - are connected to the CUT (5) inputs, and the output of the CUT(5) is fedback to the first stage of LFSR through XOR circuit. Fig. 22 represents the MSD of the system in Fig. 21. The TPM for the system is shown in Fig. 23.

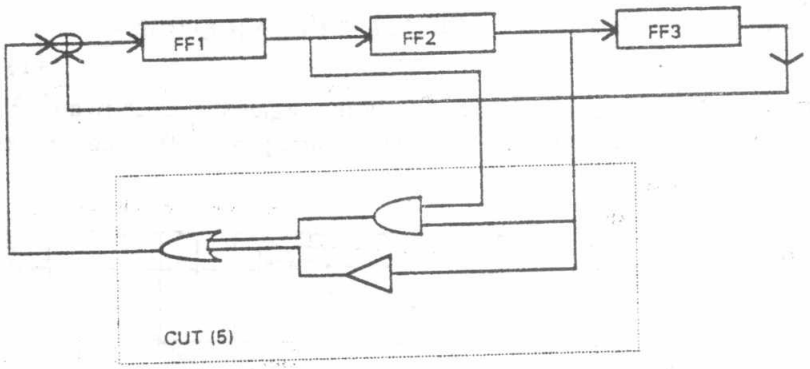

Fig. 21. CSA with LFSR, NPP, k = 3, m = 2, LSNC, CUT(5).

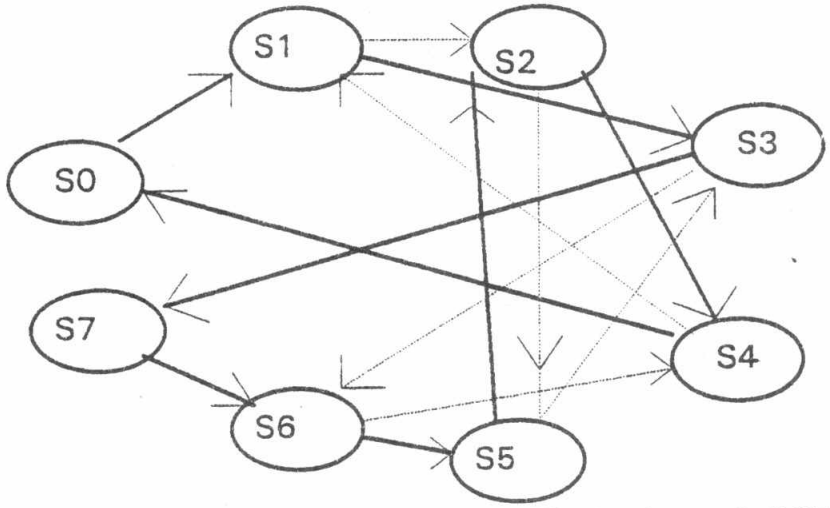

Fig. 22. MSD for CSA with LFSR, NPP, k = 3, m = 2, LSNC, CUT(5).

$$M5 = \begin{array}{c|cccccccc} & s_0 & s_1 & s_2 & s_3 & s_4 & s_5 & s_6 & s_7 \\ s_0 & 1-p & p & 0 & 0 & 0 & 0 & 0 & 0 \\ s_1 & 0 & 0 & 1-p & p & 0 & 0 & 0 & 0 \\ s_2 & 0 & 0 & 0 & 0 & p & 1-p & 0 & 0 \\ s_3 & 0 & 0 & 0 & 0 & 0 & 0 & 1-p & p \\ s_4 & p & 1-p & 0 & 0 & 0 & 0 & 0 & 0 \\ s_5 & 0 & 0 & p & 1-p & 0 & 0 & 0 & 0 \\ s_6 & 0 & 0 & 0 & 0 & 1-p & p & 0 & 0 \\ s_7 & 0 & 0 & 0 & 0 & 0 & 0 & p & 1-p \end{array}$$

Fig. 23. TPM for CSA with LFSR, NPP, k = 3, m = 2, LSNC, CUT(5).

The SME for the TPM M5 is calculated with [8]; giving :

$$SME5 = \sqrt{1-2p} \qquad (11)$$

The absolute value of SME5 is plotted against p as shown in Fig. 24. It equals zero for the case of equally likely error model when p = q = 0.5, and equal one for p = 0 or p = 1 .

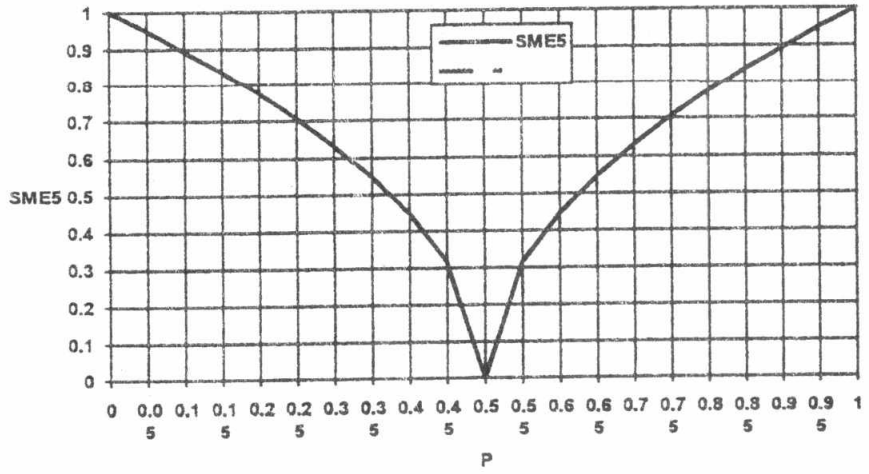

Fig. 24. Dependence of the absolute values of SME upon error probability of CUT (5) for TPM M5 of CSA with NPP-LFSR, k = 3, m = 2, LSNC.

The SME values of the CSA structure with LFSR, k = m are equal only for the case of equally likely error model when p = q = 0.5 and have the value zero, otherwise, they have different values according to the CUT and LFSR structure. On the other hand, For ICSA the general formula for SME is deduced which is independent on the CUT and LFSR structure.

4.0 Comparison Between DB of Open and Closed Loop Compaction Using LFSR :

From cases studied for the ICSA at sections (3.3), the SME for ICSA can be deduced by induction as :

$$|Z_{ICSA}| = |1-2p|^{1/2} \qquad (12)$$

The general formula for SME for PP-LFSR used in open loop system was deduced as [4],

$$|Z_{PP}| = |1-2p|^{2^{k-1}/2^k-1} \qquad (13)$$

and the general formula for SME for CC-LFSR used in open loop system was deduced as [4],

$$|Z_{NPP}| = |1-2p|^{1/k} \qquad (14)$$

Table 1 and Table 2 show the absolute values of SME for the open loop NPP-LFSR, PP-LFSR and the closed loop ICSA systems, with k = 3, and k = 5 respectively. The dependence of SME on p for k = 3, and k = 5 is plotted in Fig. 25 and Fig. 26 respectively.

p	SME of NPP-LFSR $\lvert 1-2p\rvert^{1/3}$	SME of ICSA $\lvert 1-2p\rvert^{1/2}$	SME of PP-LFSR $\lvert 1-2p\rvert^{4/7}$
0.00	1.000	1.000	1.000
0.05	0.965	0.949	0.942
0.10	0.928	0.894	0.880
0.15	0.888	0.837	0.816
0.20	0.843	0.775	0.747
0.25	0.794	0.707	0.673
0.30	0.737	0.632	0.592
0.35	0.669	0.548	0.503
0.40	0.585	0.447	0.399
0.45	0.464	0.316	0.268
0.50	0.000	0.000	0.000
0.55	0.464	0.316	0.268
0.60	0.585	0.447	0.399
0.65	0.669	0.548	0.503
0.70	0.737	0.632	0.592
0.75	0.794	0.707	0.673
0.80	0.843	0.775	0.747
0.85	0.888	0.837	0.816
0.90	0.928	0.894	0.880
0.95	0.965	0.949	0.942
1.00	1.000	1.000	1.000

Table 1. A comparison between the absolute values of SME of open loop NPP-LFSR, PP-LFSR, and ICSA for k = 3.

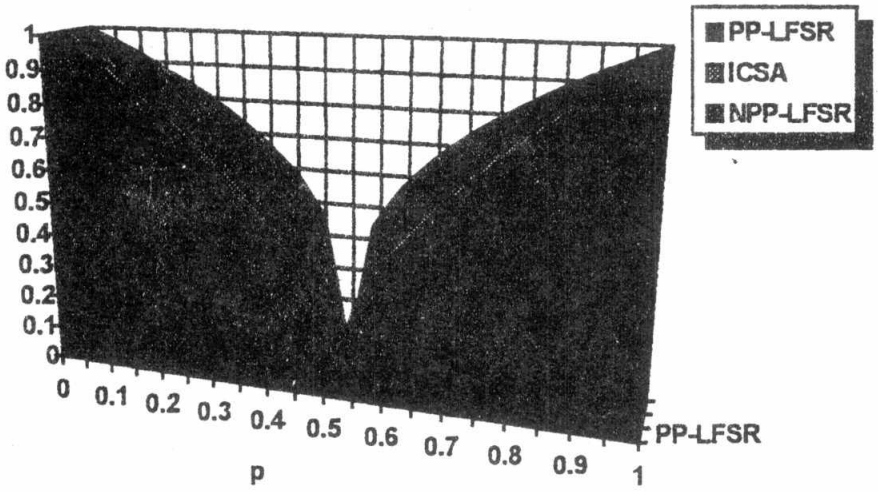

Fig.25 The SME for ICSA, PP-LFSR, and NPP-LFSR for k = 3.

p	SME of NPP-LFSR $\lvert 1-2p\rvert^{1/5}$	SME of ICSA $\lvert 1-2p\rvert^{1/2}$	SME of PP-LFSR $\lvert 1-2p\rvert^{16/31}$
0.00	1.000	1.000	1.000
0.05	0.979	0.949	0.947
0.10	0.956	0.894	0.891
0.15	0.931	0.837	0.832
0.20	0.903	0.775	0.768
0.25	0.871	0.707	0.699
0.30	0.833	0.632	0.623
0.35	0.786	0.548	0.537
0.40	0.725	0.447	0.436
0.45	0.631	0.316	0.305
0.50	0.000	0.000	0.000
0.55	0.631	0.316	0.305
0.60	0.725	0.447	0.436
0.65	0.786	0.548	0.537
0.70	0.833	0.632	0.623
0.75	0.871	0.707	0.699
0.80	0.903	0.775	0.768
0.85	0.931	0.837	0.823
0.90	0.956	0.894	0.891
0.95	0.979	0.949	0.947
1.00	1.000	1.000	1.000

Table 2. A comparison between the absolute values of SME of open loop NPP-LFSR, PP-LFSR , and ICSA for k = 5.

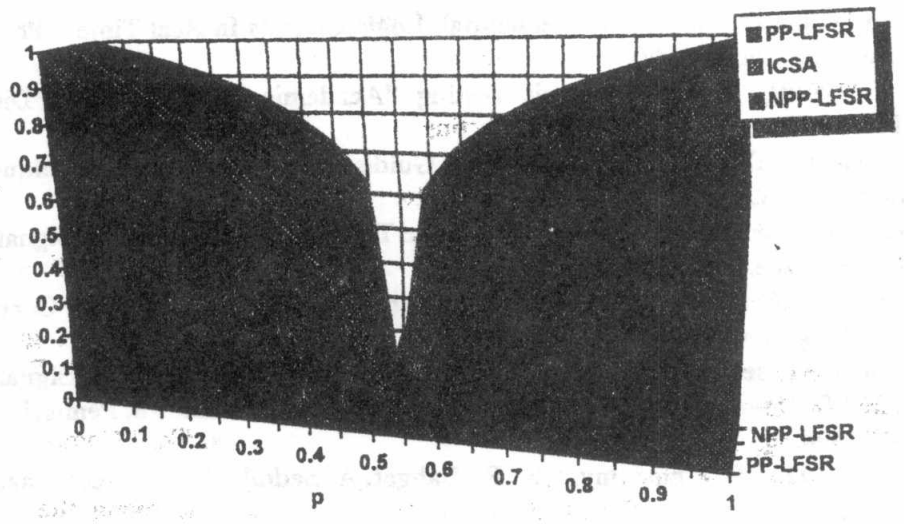

Fig. 26 The SME for ICSA, PP-LFSR, and NPP-LFSR for k = 5.

It is clear that, for p equals (1/2), the open and closed loop systems have identical SME values, equal to zero. The PP-LFSR has the minimum values of SME, which means that it needs the shortest pattern to reach the steady state values of AEP. On the other hand, ICSA needs shorter pattern than open loop NPP-LFSR, and slightly longer pattern than open loop PP-LFSR. Furthermore, as k increases the difference between the DB of the ICSA and PP-LFSR decreases.

5. Conclusions :

The dynamic behavior of CSA implemented using LFSR, with k = m and k > m have been studied, by calculating the SME value for the TPM. It was found that the SME values when p = q = 0.5 have the value zero, otherwise, they have any value between 0 and 1 , according to the CUT and LFSR structure .

The dynamic behavior of ICSA has been studied by calculating the SME values for the TPM representing the system. The general formula for SME of ICSA is deduced and compared with the general formulas for open loop systems. The comparison indicates that when the probability of the system to be fault-free is equally likely, the ICSA has similar dynamic performance like the open loop systems. But in general, the ICSA needs shorter pattern than CC-LFSR and slightly longer pattern than PP-LFSR open loop system to reach steady state, and as k increases the difference between the DB of the ICSA and PP-LFSR decreases.

These results show that the dynamic behavior of ICSA (constructed from PP-LFSR or NPP-LFSR) is nearly similar to that of the open loop PP-LFSR system for k > 5 .

References :

[1] R. Howard, " Dynamic Probabilistic System, Markov Models" J. Wiley & Sons, Inc., 1971.

[2] Stanley, W. D., Dougherty, G. R., " Digital Signal Processing " Prentice- Hall Company, 1984.

[3] W. Williams, W. Daehn, and M. Gruetzner " Comparison of Aliasing Errors For Primative and Non-Primative Polynomials" IEEE Inter. Test Conf., pp. 282 - 288, 1986

[4] R.H. Seireg "Characterization of Sequential Logic Circuits In Real Time " Ph. D. , Chicago, Illiniois , November, 1990.
[5] Francis C. Wang, " Digital Circuit Testing "Academic Press, Inc. San Diego, California 92101. 1991.
[6] France C. Wang ," Digital Circuit Testing : A Guide to DFT and Other Techniques", 1991 by Academic Press, INC.
[7] A. Seddik ," Microcomputer Based Automatic Testing System Through Signature Analysis", M. Sc Degree. M.T.C , Cairo, 1992.
[8] Mathsoft " MATHCAD 5.0 " © 1994 Mathsoft Inc. Version5.0 International Correct Spell © 1993 by Houghton Company.
[9] M. S. Ghoniemy, A. seddik," Automatic Testing of Digital Circuits Through Signature Analysis," IASTED Inter. Conf. on Modeling and Simulation, Pittsburgh, Pennsylvnia , USA. May 2-4 , 1994.
[10] R. H. Seireg, M . S. Ghoniemy, S. F. Bahgat, A. Seddik, "Compact Signature Analysis " National Conf. for Radio, Feb. 1995.
[11] M . S. Ghoniemy, R. H. Seireg, S. F. Bahgat, A. Seddik," Improving the Performance of Compact Signature Analysis Using LFSR." 13'th National Radio Science Conf. , Cairo, Egypt. 19-21 March 1996.